Contrib Mineral Petrol (2006) 152: 75–88
DOI 10.1007/s00410-006-0095-2

ORIGINAL PAPER

Hong-Fei Zhang · Li Zhang · Nigel Harris
Lan-Lan Jin · Honglin Yuan

U–Pb zircon ages, geochemical and isotopic compositions of granitoids in Songpan-Garze fold belt, eastern Tibetan Plateau: constraints on petrogenesis and tectonic evolution of the basement

Received: 31 October 2005 / Accepted: 22 March 2006 / Published online: 19 May 2006

Abstract The Songpan-Garze fold belt, located in the eastern part of the Tibetan Plateau, covers a huge triangular area bounded by the Yangtze (South China), the North China and the Tibetan Plateau blocks. In the northeastern part of the Songpan-Garze fold belt, the Yanggon and Maoergai granitoids provide insights into regional tectono-magmatic events, basement nature and tectonic evolution. U–Pb zircon SHRIMP dating shows that the Yanggon and Maoergai granitoids have magmatic crystallization ages of 221 ± 3.8 Ma and 216 ± 5.7 Ma, respectively. Both the granitoids display adakitic geochemical signatures, suggesting that their magma was derived from partial melting of thickened lower crust. Pb–Sr–Nd isotopic compositions for granitoids reveal that there is an unexposed Proterozoic basement in the Songpan-Garze belt, which has an affinity with the Yangtze block. During development of the Paleo-Tethys ocean, the basement of the Songpan-Garze belt would be a peninsula approaching the Paleo-Tethys ocean from the Yangtze block.

Communicated by J. Hoefs

H.-F. Zhang (✉) · L. Zhang · L.-L. Jin
Faculty of Earth Sciences and the State Key Laboratory of Geological Process and Mineral Resources, China University of Geosciences, Wuhan 430074, People's Republic of China
E-mail: hfzhang@cug.edu.cn
Tel.: +86-27-67883010
E-mail: lizhang@cug.edu.cn
E-mail: annjll@163.com

N. Harris
Department of Earth Sciences, The Open University, Milton Keynes MK7 6AA, UK
E-mail: n.b.w.harris@open.ac.uk

H. Yuan
The Key Laboratory of Continental Dynamics, Northwest University, Xi'an 710069, People's Republic of China
E-mail: hlyuan@nwu.edu.cn

Introduction

The Songpan-Garze fold belt is located in the eastern part of the Tibetan Plateau. The belt is a folded Triassic flysch sediment basin, which formed during closure of the Paleo-Tethys ocean (Xu et al. 1992; Mattauer et al. 1992; Sengör and Natalin 1996; Brugier et al. 1997). It covers a huge triangular area with an area of more than 200,000 km^2, bounded by the Yangtze (South China), the North China and the North Tibet (Qiantang) continental blocks (Xu et al. 1992). Therefore, the Songpan-Garze belt is a tectonic junction between numbers of the West China continental blocks and is one of the key areas for understanding the tectonic evolution of the Eurasian plate and Tibetan Plateau. It is proposed that the basement of the Songpan-Garze basin is a remnant oceanic basin (Paleo-Tethys) based on regional tectonic analysis (Zhou et al. 1993; Yin and Nie 1993). However, this assertion has not yet been confirmed by the works of others. Within the Songpan-Garze belt, granitoids are widespread. They can provide important insights into deep crustal composition and tectonic thermal event. Recently, Roger et al. (2004) carried out U–Pb zircon chronological and Sr–Nd–Pb isotopic studies of granitoids in the southeastern part of the Songpan-Garze belt. They obtained an age of 197 Ma, which was interpreted as an upper limit of the Indosinian tectonic event within the belt. The basement of the Songpan-Garze belt was suggested to have an affinity with the Yangtze continental blocks. However, previous study mainly focused on the southeastern part of the Songpan-Garze belt. In this paper, we present U–Pb zircon SHRIMP chronological data, geochemical and Sr–Nd–Pb isotopic compositions of granitoids from the northeastern part of the Songpan-Garze belt. We use the data to discuss granitoid petrogenesis, nature of basement and tectonic implications.

Geological setting

The Songpan-Garze fold belt is bounded by the Yangtze (South China), the North China and the North Tibet (Qiangdan) continental blocks (Fig. 1). To the east, the Longmenshan thrust-nappe belt separates the Songpan-Garze belt from the Sichuan basin (Xu et al. 1992; Chen et al. 1995; Chen and Wilson 1996). The northern limit of the belt is marked by the A'nimaque-Mianlue suture zone, which is considered to be a Paleo-Tethys oceanic subduction zone dipping to the north in Late Paleozoic (Sun et al. 2002; Xu et al. 2002a; Elena et al. 2003). To the southwest, the Songpan-Garze belt is bounded by the Jinshajian suture zone, which is also considered to be a Late Paleozoic Paleo-Tethys oceanic subduction zone dipping either to the west (Sengör 1985; Wang et al. 2000) or to the east (Calassou 1994).

In the Songpan-Garze belt, the sediments are almost exclusively marine Triassic flysch deposits, which reach a thickness of 5–15 km (Xu et al. 1992; Calassou 1994). The Triassic flysch sediments were intensively folded during the Indosinian (Late Triassic) compressional tectonism due to convergence between the North China, the Yangtze and the Qiangtan continental blocks (Xu et al. 1992; Brugier et al. 1997). The Triassic flysch sediments are separated from the Paleozoic sedimentary cover and the crystalline basement of the Yangtze block by a large-scale décollement near the eastern and southeastern margin of the Songpan-Garze basin (Xu et al. 1992; Mattauer et al. 1992; Calassou 1994). It was suggested that the Triassic flysch sediments were derived from denudation of the eastern China block as a result of exhumation of the Triassic ultra-high pressure metamorphic rocks in the Dabie Shan (Nie et al. 1994). This attractive hypothesis has, however, been questioned by Avigad (1995). Based on U–Pb chronological study of detrital zircons from the Triassic sediments (Brugier et al. 1997), the provenances of Middle Triassic and Upper Triassic sediments were considered to be derived from the south margin of the North China block and the Yangtze block, respectively.

Granitoids are widespread in the Songpan-Garze belt. They show sharp contact with the Triassic sediments. In the southeastern part (Markan-Wolong area) of the belt, granitoids can be divided into two groups (Roger et al. 2004): Group One is amphibolite granites (197 ± 6 Ma, U–Pb zircon), resulted from partial melting of the Yangtze basement below the Songpan-Garze décollement level during the Indosinian tectonic event, whereas Group Two is biotite and/or muscovite granites (188 ± 2 Ma and 153 ± 3 Ma, U–Pb zircon),

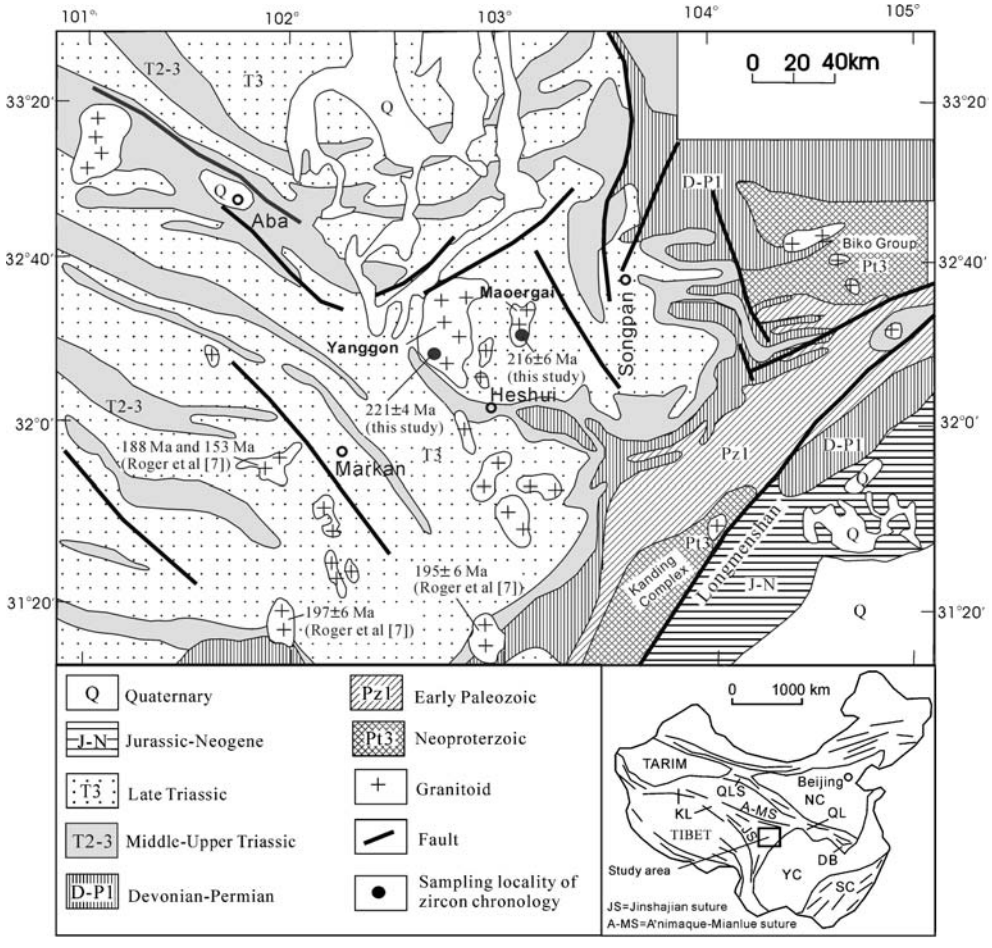

Fig. 1 Simplified geological map of the northeast part of Songpan-Garze fold belt. *Inset* shows location of study area. NC = North China block, YC = Yangtze block, SC = South China fold belt, KL = Kunlan Mountains, QLS = Qillian Mountains, QL = Qinling Mountains, DB = Dabieshan

which resulted from the partial melting of the Middle Triassic sediments after the tectonic event.

In the northeastern part of the Songpan-Garze belt, a detailed chronological and geochemical study is still lacking. Two of the granitoid plutons (the Yanggon and the Maoergai plutons) have been sampled for this study (Fig. 1). Both intrude the folded Triassic sediments.

The Yanggon pluton with an area of ~1,050 km^2 comprises medium-grained and undeformed rocks, ranging in composition from granodirite to granite. The granodiorite is a predominant rock type in this pluton. In the field, a sharp contact between the granodirite and the granite has not been observed, indicating that they are coeval. The granodirite contains 15–20% quartz, 40–50% plagioclase (An = 25–35), 15–20% K-feldspars, 3–6% biotite and 1–2% hornblende. The granite consists of 20–24% quartz, 35–40% plagioclase (An = 18–25), 20–35% K-feldspars, 1–3% biotite and 0–1% muscovite. Both the granodiorite and granite have a similar accessory mineral assemblage of magnetite, sphene, zircon, monazite and apatite.

Forty kilometers eastwards of the Yanggon pluton lies the undeformed Maoergai pluton with an area of ~60 km^2. This pluton has uniform petrography. It comprises fine–medium grained granite with 20–25% quartz, 35–45% plagioclase (An = 20–30), 25–30% K-feldspars and 2–4% biotite, accessory minerals including magnetite, zircon, monazite and apatite.

Analytical methods

For U–Pb zircon dating, zircons were separated from rock samples using conventional techniques at China University of Geosciences. The zircon crystals together with the zircon standard Temora (Black 2003) were mounted in an epoxy disc and then polished to expose their centres. The internal structure for the zircons was observed using CL and BSE images. Under guidance of zircon CL images, the zircons were analyzed for U–Pb isotopes and U, Th and Pb concentrations using SHRIMP II at the Beijing SHRIMP Centre, Institute of Geology, CAGS. The analysis follows Compston et al. (1992) and Williams and Claesson (1987). Measurements were corrected using reference zircon standard SL13 (572 Ma) and zircon standard Temora (417 Ma). The reference zircon was analyzed for every fourth analysis. The common Pb was estimated from ^{204}Pb counts, and the data processing is carried out using Isoplot (Ludwig 1997). Ages are weighted means with 2σ errors.

Analyses of major element compositions were made at the Key Laboratory of Continental Dynamics, Northwest University (Xi'an, China) by XRF. The analytical uncertainty is usually < 5%. Trace elements and rare earth elements (REE) were measured using ICP-MS at China University of Geosciences. The analytical precision is better than 5–10%. For a detailed analytical method, see Zhang et al. (2002).

Whole-rock Sr–Nd isotopic data were obtained using a Finnigan Triton multi-collector mass spectrometer at Open University, UK. Sr and Nd isotopic fractionations were corrected to $^{86}Sr/^{88}Sr = 0.1194$ and $^{146}Nd/^{144}Nd = 0.7219$, respectively. During the period of analysis, NBS987 standard yielded an average value of $^{87}Sr/^{86}Sr = 0.710244 \pm 14$ (2σ) and the Johnson-Matthey internal standard and BCR-2 standard gave average values of $^{143}Nd/^{144}Nd = 0.511825 \pm 6$ (2σ) and $^{143}Nd/^{144}Nd = 0.512644 \pm 6$ (2σ), respectively. Total procedural Sr and Nd blanks are < 4 ng and < 1 ng, respectively. Details are given in Zhang et al. (2004).

Whole-rock Pb was separated by an anion exchange in HCl–Br columns at China University of Geosciences. Pb isotopic ratios were measured by Nu Plasma ICP-MS at the Key Laboratory of Continental Dynamics, Northwest University. Pb isotopic fractionation was corrected to $^{205}Tl/^{203}Tl = 2.3875$. Within the analytical period, 30 measurements of NBS981 gave average values of $^{206}Pb/^{204}Pb = 16.937 \pm 1\,(2\sigma)$, $^{207}Pb/^{204}Pb = 15.491 \pm 1$ and $^{208}Pb/^{204}Pb = 36.696 \pm 1$. BCR-2 standard gave $^{206}Pb/^{204}Pb = 18.742 \pm 1\,(2\sigma)$, $^{207}Pb/^{204}Pb = 15.620 \pm 1$ and $^{208}Pb/^{204}Pb = 38.705 \pm 1$. Total procedural Pb blanks were in the range of 0.1–0.3 ng.

Results

U–Pb zircon SHRIMP ages

U–Pb zircon SHRIMP data are listed in Table 1, and representative zircon CL images and spot analyses are shown in Fig. 2.

Zircons from the Yanggon granitoid (sample Y-4) are dominated by light pink to colourless euhedral crystals. They have perfect pyramids and prisms. The zircons range in length from ~100 to ~250 μm with length/width ratios from 2:1 to 4:1. The zircon CL images (Fig. 2a) exhibit good oscillatory zoning, indicative of magma zircons. Some zircons contain the core of inherited zircon. Twelve spot analyses (not including inherited zircons) show that 11 points are mostly concordant within error and one point is discordant (Fig. 3a). The discordant point could be resulted from uncertainty of measured $^{207}Pb/^{235}U$ ratio due to low ^{207}Pb. All points have $^{206}Pb/^{238}U$ ages ranging from 215 to 232 Ma with a weighted mean age of 221 ± 3.8 Ma (2σ; MSWD = 0.66), which is interpreted as the magma crystallization age of the Yanggon pluton.

Zircons from the Maoergai granite (sample M-2) are pink to colourless. They exhibit well-developed crystal faces. Most zircons have length/width ratios from 2:1 to 3:1 and a few zircons have length/width ratios close to 4:1. They have subtle magmatic oscillatory zoning in CL images (Fig. 2b). Some zircons display the core of inherited zircon. Ten spot analyses (not including inherited zircons) display that they are mostly concordant

Table 1 SHRIMP zircon analytical data

Analysis	^{206}Pbc[a] (%)	U (ppm)	Th (ppm)	$^{232}Th/^{238}U$	$^{206}Pb*$[b] (ppm)	age (Ma)[c] $^{206}Pb/^{238}U$	± 2σ	age (Ma)[c] $^{207}Pb/^{206}Pb$	± 2σ	age (Ma)[c] $^{208}Pb/^{232}Th$	± 2σ	$^{206}Pb*/^{238}U$	± %	$^{207}Pb*/^{235}U$	± %
Yanggon granodiritre: sample Y-4															
Y41.1	0.25	983	141	0.15	29.9	223.7	6.8	146	55	214	13	0.0353	3.1	0.2426	3.5
Y42.1	0.25	1359	239	0.18	41.8	226.1	6.9	189	46	222	10	0.0357	3.1	0.2475	3.4
Y43.1	0.10	1113	358	0.33	33.5	221.8	6.8	267	51	224	9.0	0.0350	3.1	0.2465	3.4
Y44.1	0.26	1011	206	0.21	29.5	214.9	6.6	264	65	213	13	0.0339	3.1	0.2421	3.5
Y45.1	0.06	973	142	0.15	29.2	221.3	6.8	297	38	251	9.8	0.0349	3.1	0.2386	3.6
Y46.1	0.30	903	154	0.18	27.6	225.0	7.2	760	42	370	16	0.0355	3.3	0.2411	3.8
Y47.1	0.04	1228	212	0.18	37.3	223.7	7.0	267	48	250	10	0.0353	3.2	0.2374	3.8
Y48.1	0.10	839	142	0.17	26.4	231.5	7.1	406	36	273	11	0.0366	3.1	0.2552	3.5
Y49.1	0.14	1123	247	0.23	33.1	217.0	6.6	249	34	220	7.8	0.0342	3.1	0.2396	3.4
Y410.1	0.23	991	140	0.15	30.1	223.3	6.8	428	57	297	18	0.0353	3.1	0.2378	3.6
Y411.1	0.09	1368	344	0.26	39.4	212.2	6.5	220	35	210	7.2	0.0335	3.1	0.2349	3.4
Y412.1	0.31	941	161	0.18	27.6	215.7	6.6	169	65	212	14	0.0340	3.1	0.2339	3.5
Maoergai granite: sample M-2															
M21.1	0.41	953	224	0.24	27.7	213.4	6.3	314	72	226	13	0.0337	3.0	0.2440	4.4
M22.1	0.27	5206	814	0.16	148	209.9	6.3	296	30	232	9.3	0.0331	3.1	0.2384	3.3
M23.1	1.44	439	97	0.23	12.5	207.9	6.4	152	210	218	32	0.0328	3.1	0.2220	9.7
M24.1	0.08	4880	627	0.13	139	209.6	6.1	209	23	216	7.7	0.0331	3.0	0.2292	3.1
M25.1	0.12	2890	5693	2.04	83.8	213.8	6.2	187	30	206	6.2	0.0337	2.9	0.2317	3.2
M26.1	0.09	11336	82	0.01	348	225.9	7.2	230	22	137	43	0.0357	3.2	0.2496	3.4
M27.1	0.22	2585	318	0.13	78.1	222.4	6.5	262	31	216	8.1	0.0351	3.0	0.2491	3.3
M28.1	0.22	6417	336	0.05	193	221.1	6.6	280	30	247	14	0.0349	3.0	0.2496	3.3
M29.1	0.99	14913	1541	0.11	476	232.9	6.7	283	24	242	11	0.0368	2.9	0.2635	3.1
M210.1	1.15	2123	161	0.08	61.9	212.8	6.2	443	80	295	36	0.0336	3.0	0.2580	4.7

[a]Common portion
[b]Radiogenic portion
[c]Corrected using measured ^{204}Pb

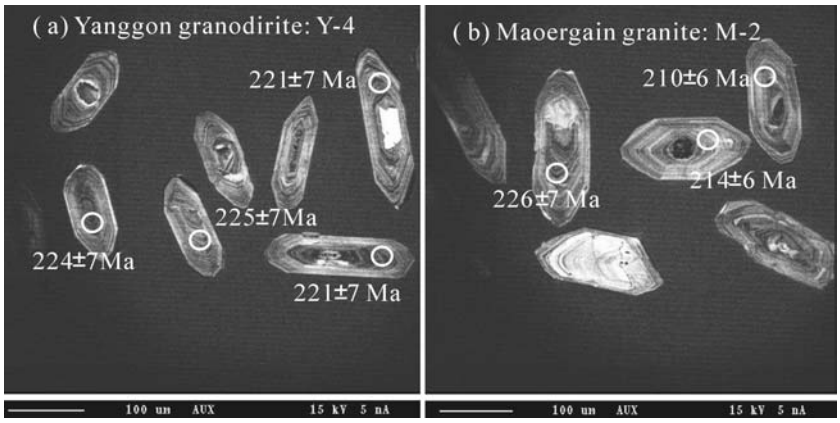

Fig. 2 Representative zircon CL image and SHRIMP spot analysis. **a** Yanggon granodirite (sample Y-4), **b** Maoergai granite (sample M-2). The zircon CL images from the both samples show good magmatic oscillatory zoning, indicating that the analysed zircon U–Pb ages represent their magma crystallization ages

(Fig. 3a). They have $^{206}Pb/^{238}U$ ages ranging from 208 to 233 Ma with an average age of 216 ± 5.7 Ma (MSWD = 1.67), which is interpreted as the magma crystallization age of the Maoergai pluton.

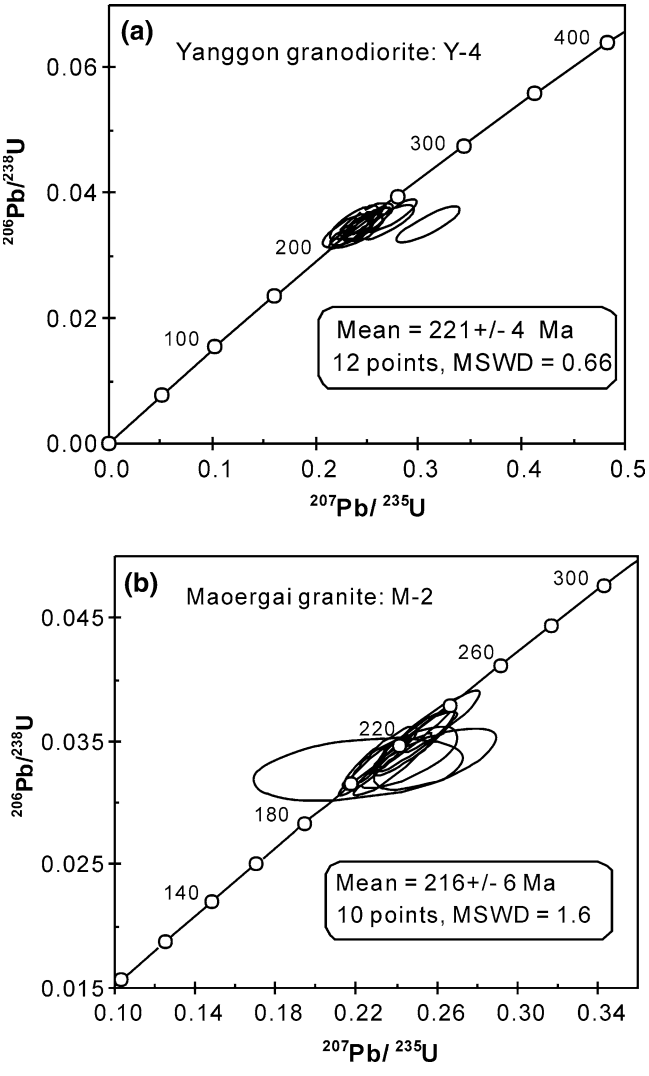

Fig. 3 Zircon U–Pb concordia diagram. **a** Yanggon granodirite, **b** Maoergai granite

Major and trace elements

Major and trace elemental compositions for the Yanggon and the Maoergai granitoids in the Songpan-Garze belt are given in Table 2.

The Yanggon granitoids (eight samples) display SiO_2 = 66.90–74.15%, Al_2O_3 = 13.97–15.43%, MgO = 0.34–1.18%, CaO = 1.29–4.15%, Fe_2O_3 + FeO = 1.17–4.06% and K_2O = 3.36–4.28% with K_2O/Na_2O = 1.06–1.42. The Maoergai granites (four samples) have SiO_2 = 70.63–74.09%, Al_2O_3 = 14.07–14.92%, MgO = 0.24–0.67%, CaO = 1.64–3.34%, Fe_2O_3 + FeO = 1.03–2.39% and K_2O = 3.38–4.48% with K_2O/Na_2O = 0.86–1.39. The major element compositions of the Maoergai granitoids largely overlap with those of the Yanggon granitoids. In Harker diagram (Fig. 4), the chemical compositions from the Yanggon and the Maoergai granitoids display co-linear variation trends: TiO_2, Al_2O_3, FeO, MgO and CaO decrease with increasing SiO_2. This might imply that both the plutons have similar petrogenesis and magma evolution. A/CNK values [molar $Al_2O_3/(CaO + Na_2O + K_2O)$] range from 0.94 to1.05 for the Yanggon granitoids and from 0.97 to 1.01 for the Maoergai granitoids, indicating that they are dominantly metaluminous.

Trace element data (Table 2) show that the Yanggon and Maoergai granitoids have a large variation of trace element contents. The Yanggon granitoids display Rb = 106–380 ppm, Sr = 178–1,003 ppm, Ba = 443–1,481 ppm, Zr = 99–232 ppm, Hf = 2.41–6.51 ppm, Y = 6.6–13.2 ppm, Nb = 6.5–16.2 ppm and Ta = 0.53–1.38 ppm. The Maoergai granitoids display Rb = 141–189 ppm, Sr = 474–854 ppm, Ba = 842–1,238 ppm, Zr = 87–190 ppm, Hf = 2.54–5.57 ppm, Y = 8.92–9.73 ppm, Nb = 8.1–13.6 ppm and Ta = 0.96–1.54 ppm. Although the Yanggon and Maoergai granitoids exhibit a large variation in trace element contents, they have similar primitive mantle-normalized trace element patterns (Fig. 5). All samples display negative Nb, P and Ti anomalies without Zr and Hf anomalies. Most of the samples have weak Sr positive anomaly. Rare earth element (REE) data show that the Yanggon and Maoergai granitoids have

Table 2 Data of major elements (%) and trace elements (ppm)

Samples	Y-1	Y-2	Y-3	Y-4	Y-5	Y-6	Y-7	Y-8	M-1	M-2	M-3	M-4
SiO_2	66.9	67.44	67.29	72.64	74.15	70.06	69.43	69.49	74.09	70.63	72.53	71.35
TiO_2	0.59	0.54	0.59	0.32	0.21	0.49	0.5	0.5	0.2	0.41	0.29	0.37
Al_2O_3	15.43	15.19	15.27	14.24	13.97	14.86	15.02	14.85	14.07	14.92	14.15	14.63
TFeO	4.06	3.73	4.05	1.63	1.17	2.95	2.88	3.08	1.03	2.39	1.65	2.22
MnO	0.08	0.07	0.07	0.02	0.01	0.04	0.04	0.04	0.02	0.04	0.02	0.04
MgO	1.18	1	1.14	0.42	0.34	0.79	0.8	0.75	0.24	0.64	0.58	0.67
CaO	4.15	3.87	4.04	1.29	2.25	3.43	3.57	3.15	1.64	3.34	2.1	2.71
Na_2O	3.13	3.25	3.08	3.98	3.43	2.83	2.79	2.95	4.28	3.43	3.22	3.34
K_2O	3.36	3.44	3.42	4.28	3.89	3.42	3.47	4.2	3.69	3.38	4.48	3.86
P_2O_5	0.23	0.22	0.23	0.21	0.06	0.16	0.16	0.18	0.06	0.12	0.12	0.12
Lost	0.52	0.9	0.45	0.78	0.38	0.7	1.08	0.48	0.42	0.4	0.65	0.42
Total	99.63	99.65	99.63	99.81	99.86	99.73	99.74	99.67	99.74	99.7	99.79	99.73
K_2O/Na_2O	1.07	1.06	1.11	1.08	1.13	1.21	1.24	1.42	0.86	0.99	1.39	1.16
A/CNK	0.94	0.94	0.95	1.05	1.00	1.02	1.01	0.98	1.00	0.97	1.01	1.00
Be	3.32	3.44	3.24	6.01	3.76	4.15	3.78	3.74	7.43	4.11	6.71	3.83
Sc	7.90	6.68	7.33	2.17	2.27	4.52	4.61	6.49	1.75	3.66	4.25	4.76
V	60.90	48.72	58.68	13.36	9.54	33.73	30.66	26.16	3.42	19.57	17.07	21.53
Cr	17.04	8.11	11.15	8.69	8.58	5.40	8.06	6.90	7.03	4.96	12.23	7.71
Co	4.73	3.92	4.50	2.69	1.64	3.15	3.38	3.33	1.19	2.45	1.95	2.88
Ni	8.46	2.80	2.95	4.35	4.50	2.14	3.13	2.10	5.33	1.95	3.48	2.37
Cu	8.54	7.98	5.27	5.04	3.35	3.74	13.68	10.70	2.02	6.40	4.62	7.80
Zn	75.88	74.05	74.37	75.41	37.26	70.38	78.53	94.33	36.85	75.14	50.93	67.39
Ga	19.35	18.55	18.64	26.47	20.58	21.23	22.23	23.45	22.37	21.94	22.36	23.36
Rb	113	114	106	380	128	132	133	154	189	141	180	164
Sr	1003	963	955	178	734	633	650	934	562	854	474	674
Y	12.21	13.22	12.81	8.42	6.62	11.00	11.94	10.94	8.92	9.73	9.47	8.93
Zr	118	158	160	150	99	156	169	232	87	190	134	179
Nb	16.22	14.78	14.94	13.88	6.52	13.75	14.46	15.14	8.09	13.61	11.31	11.32
Cs	4.92	8.47	5.28	36.33	5.99	9.61	7.20	6.06	10.06	9.76	17.19	11.31
Ba	1481	1410	1401	443	1057	1023	950	1446	960	1238	842	1122
Hf	3.78	5.40	5.33	3.62	2.41	4.77	5.20	6.51	2.54	5.57	4.50	5.15
Ta	1.38	1.28	1.33	1.36	0.53	1.17	1.31	1.03	1.14	1.18	1.54	0.96
Pb	36.80	39.57	36.69	31.19	27.85	30.10	32.91	33.23	32.02	37.63	45.43	36.59
Th	16.78	16.98	16.44	26.66	5.86	11.22	11.14	19.07	10.57	13.32	12.00	14.44
U	3.18	3.48	3.61	2.37	1.19	2.70	3.57	1.95	1.82	3.24	3.08	2.94
Sr/Y	82.13	72.85	74.59	21.13	110.81	57.52	54.42	85.39	63.03	87.72	50.01	75.46
La	56.54	52.20	51.18	48.01	16.62	35.23	34.49	60.52	23.61	40.13	30.18	41.41
Ce	94.84	87.08	88.14	84.09	29.10	61.01	59.51	100.91	38.55	64.26	48.45	64.70
Pr	11.52	10.28	10.51	8.69	2.94	8.09	7.79	11.80	3.82	7.56	5.68	7.44
Nd	43.90	39.08	39.65	32.41	11.29	30.15	30.20	42.64	13.36	26.59	20.13	25.82
Sm	7.44	6.66	6.96	5.97	2.18	5.45	5.27	6.55	2.56	4.20	3.48	3.92
Eu	1.85	1.61	1.69	0.73	0.63	1.26	1.33	1.46	0.56	1.17	0.88	1.00
Gd	6.58	5.18	6.12	4.13	1.81	4.33	4.24	5.17	2.10	3.39	2.79	3.29
Tb	0.78	0.68	0.68	0.46	0.24	0.57	0.59	0.59	0.30	0.43	0.39	0.38
Dy	4.29	3.82	4.11	1.59	0.89	2.61	2.77	2.59	1.43	2.04	1.90	1.82
Ho	0.77	0.67	0.78	0.23	0.19	0.40	0.42	0.37	0.24	0.32	0.31	0.28
Er	2.09	1.97	2.10	0.50	0.41	0.95	1.03	0.88	0.52	0.84	0.82	0.72
Tm	0.27	0.26	0.28	0.07	0.06	0.12	0.12	0.10	0.08	0.10	0.11	0.10
Yb	1.83	1.70	1.77	0.46	0.38	0.73	0.80	0.69	0.52	0.73	0.69	0.66
Lu	0.32	0.28	0.29	0.06	0.06	0.10	0.10	0.10	0.07	0.10	0.09	0.09
(La/Yb)N	26.94	27.38	25.60	70.55	29.77	32.41	29.04	59.39	30.62	37.30	29.51	42.62
Eu*/Eu	0.79	0.81	0.77	0.43	0.93	0.76	0.83	0.74	0.72	0.91	0.83	0.83

Y = Yanggon granitoid, M = Maoergai granite

similar strongly fractionated patterns (Fig. 6), with $(La/Yb)_N$ of 25.60–70.55, 29.51–42.62 and Eu*/Eu of 0.43–0.93, 0.72–0.91, respectively. The high ratios of $(La/Yb)_N$ and low values of Yb_N (1.8–6.8) for both the granitoids suggest that their magma source contain residual garnet characterized by low LREE/HREE ratios and high HREE contents.

Sr–Nd–Pb isotopes

Whole-rock Sr–Nd isotopic data for the Yanggon and Maoergai granitoids are presented in Table 3.

Initial Sr isotopic ratio Isr and Nd isotopic parameter $\varepsilon_{Nd}(t)$ are calculated at t = 220 Ma. The Yanggon granitoids (seven samples) have I_{Sr} = 0.7061–0.7082

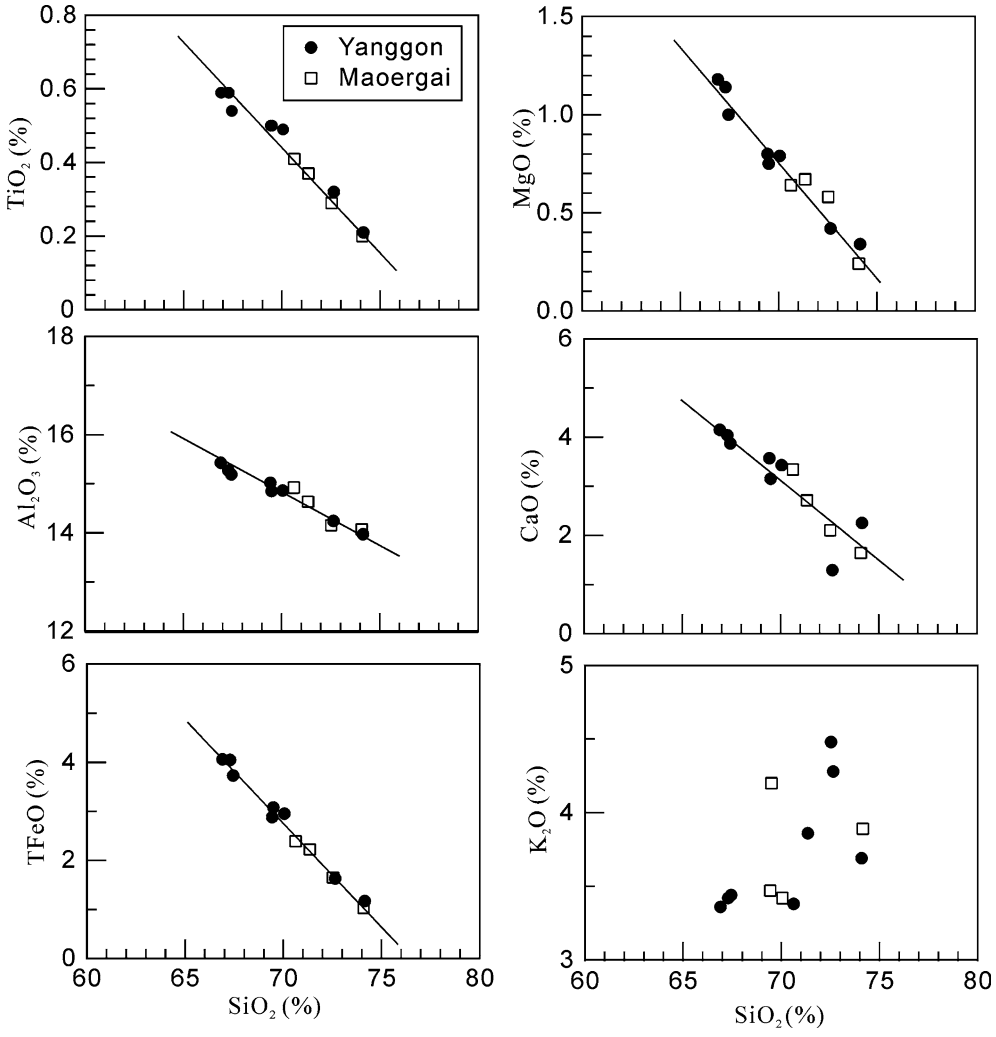

Fig. 4 Harker diagram showing content variation of major elements

and $\varepsilon_{Nd}(t) = -6.0$ to -9.5. Nd isotopic model ages (T_{DM}) range from 1.31 to 1.65 Ga. The Maoergai granitoids (three samples) display $I_{Sr} = 0.7068$–0.7078 and $\varepsilon_{Nd}(t) = -6.0$ to -7.4 with $T_{DM} = 1.25$–1.55 Ga. The results show that the Yanggon and Maoergai granitoids have similar Sr and Nd isotopic compositions, indicating that they share a common magma source, which is recycled continental crustal material without significant mantle-source contribution.

Whole-rock Pb isotopic data (Table 4) show that the Yanggon and Maoergai granitoids also have similar Pb isotopic composition. All samples are characterized by high radiogenic Pb isotopic composition with present-day whole-rock Pb isotopic ratios of $^{206}Pb/^{204}Pb = 18.331$–$18.803$, $^{207}Pb/^{204}Pb = 15.636$–$15.694$ and $^{208}Pb/^{204}Pb = 38.528$–$39.118$. According to the whole-rock Pb isotopic ratios and whole-rock U, Th and Pb contents, the initial Pb isotopic ratios of the Yanggon and Maoergai granitoids at t = 220 Ma are calculated using a single stage Pb isotopic evolution model (Zartman and Doe 1981). The calculated initial Pb isotopic ratios are $(^{206}Pb/^{204}Pb)_t = 18.191$–$18.624$, $(^{207}Pb/^{204}Pb)_t = 15.628$–$15.685$ and $(^{208}Pb/^{204}Pb)_t = 38.317$–$38.480$, which are not significantly different from the present-day Pb isotopic ratios (Table 4) because of their young age and relatively low Th and U concentrations.

Discussions

Petrogenesis

The Yanggon and Maoergai granitoids have similar U–Pb zircon ages, geochemical and Sr–Nd–Pb isotopic compositions. Therefore, both the granitoids have similar petrogenesis and magma source. Relative to normal *I*- and *S*-type granitoids (White and Chappell 1977), the Yanggon and Maoergai granitoids are depleted in Y (< 14 ppm) and HREE (eg. Yb < 1.85 ppm) and enriched in Sr (up to 1,003 ppm) with weak positive Sr anomaly in primitive mantle-normalized trace element patterns (Fig. 5). They have high $(La/Yb)_N$ (25.6–70.6) and Sr/Y (21–111) ratios. Thus, the Yanggon and Maoergai granitoids are high Sr and low Y granitoids. This type of granitoid is the first identification in the

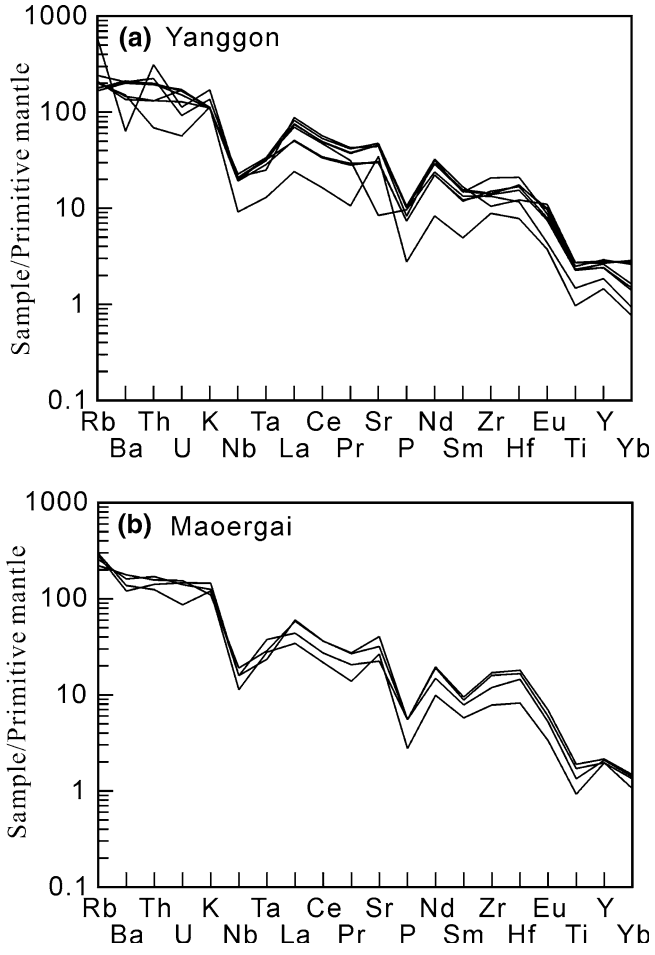

Fig. 5 Primative mantle normalized trace element spider diagram. **a** Yanggon granodirite, **b** Maoergai granite. Normalizing values from Sun and McDonough (1989)

Songpan-Garze belt. The geochemical signatures of the Yanggon and Maoergai granitoids are comparable to TTG and adakite as defined by Defant and Drummond (1990). As shown in Figs. 7 and 8, all samples from the Yanggon and Maoergai granitoids fall in the field of adakite.

For adakitic magma generation, there are several possible origins by partial melting of (1) subducted oceanic slab (Defant and Drummond 1990; Peacock et al. 1994; Drummond et al. 1996; Sajona et al. 2000; Gutscher et al. 2000; Beate et al. 2001), (2) underplating basaltic lower crust (Atherton and Petord 1993; Muir et al. 1995; Barnes et al. 1996; Petford and Atherton 1996), and (3) delerminated lower crust (Xu et al. 2002b; Gao et al. 2004; Wang et al. 2006) or thickened lower crust (Chung et al. 2003; Hou et al. 2004; Wang et al., 2005). Experimental studies show that the magma source for adakite results from a basaltic source transformed to garnet amphibolite and/or amphibole eclogite at pressures equivalent to a thickness > 50 km (Sen and Dunnt 1994; Rapp et al. 1995). Therefore, crustal thickening is essential for petrogenesis of adakitic rocks with crustal isoptoic characteristics.

The Yanggon and Maoergai granitoids have K_2O/Na_2O ratios of 0.86–1.42, low MgO (0.23–1.18%), Cr (4.96–17.04 ppm), Co (1.19–4.73 ppm) and Ni (1.95–8.46 ppm) contents and evolved Sr–Nd isotopic composition, showing that they are distinct from some adakites, resulted from partial melting of subducted oceanic slab, underplated basaltic lower crust and delaminated lower crust. The Yanggon and Maoergai granitoids have slightly high Isr (0.7061–0.7082) and negative $\varepsilon_{Nd}(t)$ values (−6.0 to −9.5) with T_{DM} = 1.31–1.65 Ga, indicating that their magma source was predominantly derived from Precambrian continental crustal material and mantle source contribution can be neglected. Therefore, a thickened crustal model (Chung et al. 2003; Hou et al. 2004; Wang et al. 2005) for adakitic magma generation can account for the petrogenesis of the adakitic Yanggon and Maoergai granitoids. This is in agreement with convergence between the North China, Yangtze (South China) and Qiangtan continental blocks during the Indosinian compressional tectonic event (Zhang et al. 2000). According to generation depth of adakitic magma (Sen and Dunnt 1994; Rapp et al. 1995), we suggest that the crust of the Songpan-Garze belt was thickened to > 50 km in the

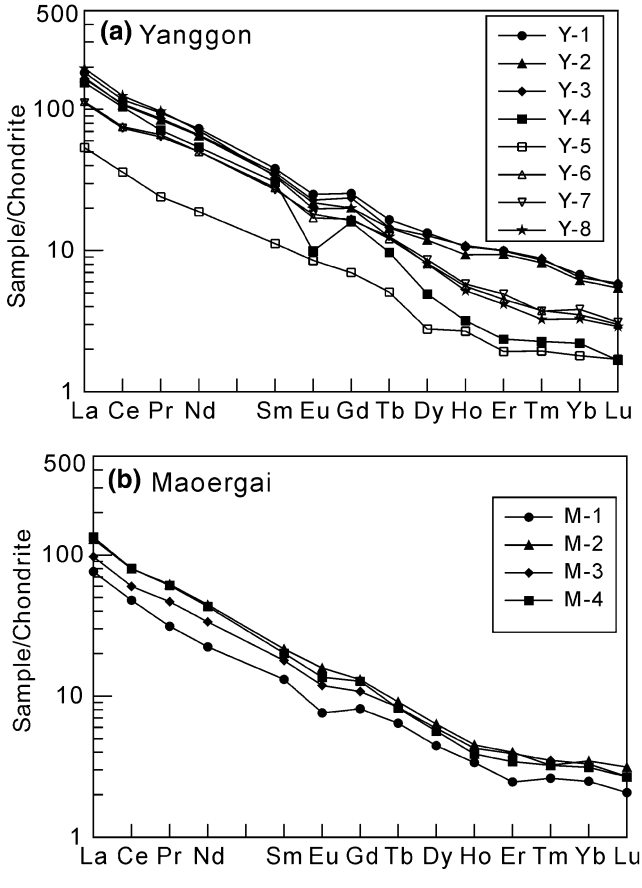

Fig. 6 Chondrite-normalized REE patterns. **a** Yanggon granodirite, **b** Maoergai granite. Normalizing values are from Taylor and McLennan (1985)

Table 3 Data of whole-rock Sr and Nd isotopes

Sample	$^{87}Rb/^{86}Sr$[a]	$^{87}Sr/^{86}Sr$	$\pm 2\sigma$	I_{Sr}(220Ma)	$^{147}Sm/^{144}Nd$[a]	$^{143}Nd/^{144}Nd$	$\pm 2\sigma$	ε_{Nd}(220 Ma)[b]	T_{DM}(Ga)[c]
Y-1	0.326	0.70830	1	0.7073	0.102	0.512185	6	−6.2	1.32
Y-2	0.344	0.70827	1	0.7072	0.103	0.512197	6	−6.0	1.31
Y-3	0.322	0.70810	1	0.7071	0.106	0.512201	5	−6.0	1.34
Y-4	6.190	0.72745	1	0.7082	0.111	0.512193	8	−6.3	1.42
Y-5	0.507	0.70796	1	0.7064	0.117	0.512101	6	−8.2	1.65
Y-6	0.606	0.70801	1	0.7061	0.109	0.512027	6	−9.5	1.64
Y-8	0.477	0.70917	1	0.7077	0.093	0.512105	4	−7.5	1.32
M-1	0.975	0.70984	1	0.7068	0.116	0.512153	6	−7.2	1.55
M-2	0.478	0.70930	1	0.7078	0.095	0.512183	4	−6.0	1.25
M-4	0.705	0.70995	1	0.7078	0.092	0.512108	4	−7.4	1.30

[a] $^{87}Rb/^{86}Sr$ and $^{147}Sm/^{144}Nd$ ratios are calculated using Rb, Sr, Sm and Nd contents (Table 2), measured by ICP-MS
[b] $\varepsilon_{Nd}(t)$ values are calculated using present-day $(^{147}Sm/^{144}Nd)_{CHUR} = 0.1967$ and $(^{143}Nd/^{144}Nd)_{CHUR} = 0.512638$
[c] T_{DM} values are calculated using present-day $(^{147}Sm/^{144}Nd)_{DM} = 0.2137$ and $(^{143}Nd/^{144}Nd)_{DM} = 0.51315$

Table 4 Whole-rock Pb isotopic data

Sample	$^{206}Pb/^{204}Pb \pm 2\sigma$	$^{207}Pb/^{204}Pb \pm 2\sigma$	$^{208}Pb/^{204}Pb \pm 2\sigma$	$^{238}U/^{204}Pb$[a]	$^{232}Th/^{204}Pb$[a]	$(^{206}Pb/^{204}Pb)_t$[b]	$(^{207}Pb/^{204}Pb)_t$[b]	$(^{208}Pb/^{204}Pb)_t$[b]
Y-1	18.390 ± 1	15.638 ± 1	38.680 ± 2	5.50	30.0	18.191	15.628	38.336
Y-2	18.435 ± 1	15.639 ± 1	38.669 ± 2	5.61	28.3	18.231	15.628	38.345
Y-4	18.803 ± 1	15.694 ± 1	39.118 ± 3	4.91	57.0	18.624	15.685	38.466
Y-5	18.331 ± 1	15.641 ± 1	38.528 ± 4	2.72	13.8	18.233	15.636	38.369
Y-6	18.479 ± 1	15.658 ± 1	38.762 ± 3	5.73	24.6	18.271	15.648	38.480
Y-8	18.498 ± 1	15.639 ± 1	38.831 ± 2	3.75	37.9	18.362	15.632	38.397
M-1	18.542 ± 1	15.655 ± 1	38.690 ± 3	3.63	21.8	18.410	15.649	38.440
M-2	18.403 ± 1	15.636 ± 1	38.584 ± 3	5.48	23.3	18.204	15.625	38.317
M-4	18.512 ± 1	15.654 ± 1	38.771 ± 2	5.14	26.1	18.325	15.645	38.473

[a] Calculated by measured whole-rock U, Th and Pb contents (Table 2) and present-day whole-rock Pb isotopic ratios
[b] Initial Pb isotopic ratio at t = 220 Ma, calculated using single-stage model

Late Triassic. The partial melting of the thickened Songpan-Garze lower crust generated the magma of the adakitic Yanggon and Maoergai granitoids. Source residual minerals contain garnet. This can account for the geochemical characteristics of the adakitic Yanggon and Maoergai granitoids.

Nature of basement

Identification of the magma source for the Yanggon and Maoergai granitoids is critical to understanding the nature of the basement. Because both the granitoids intrude into the low-grade metamorphic Triassic flysch

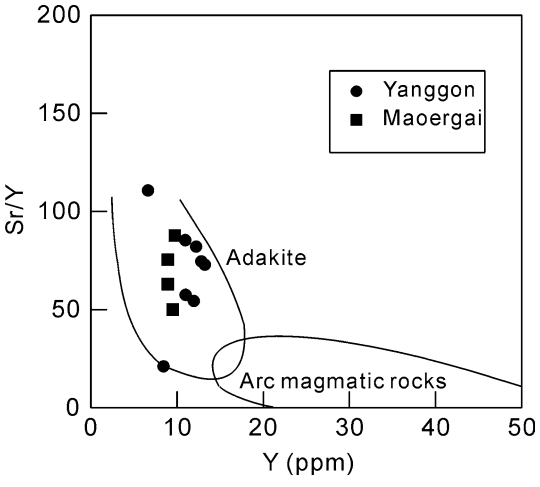

Fig. 7 Sr/Y versus Y diagram. Field of adakite is from Defant and Drummond (1990)

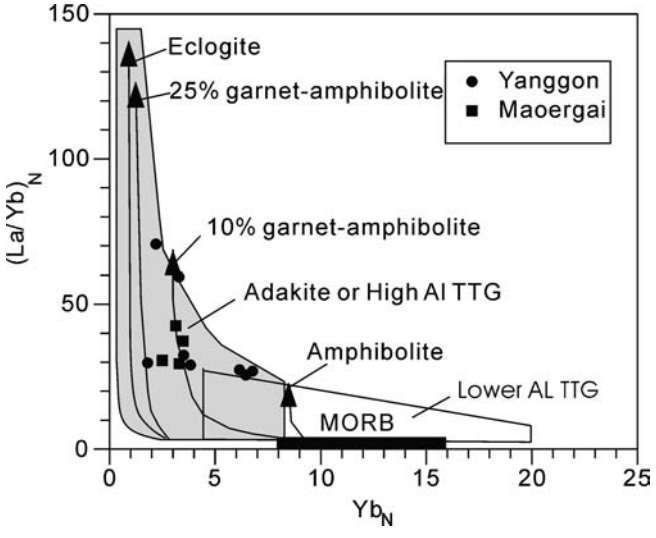

Fig. 8 $(La/Yb)_N$ versus Yb_N diagram. Field of adakite is from Defant and Drummond (1990)

sediments, it is unlikely for the Triassic flysch sediments to be the dominant magma source for the Yanggon and Maoergai granitoids. Therefore, their magma source would be from deep continental crust underlying the Triassic flysch sediments. This implies that there is an unexposed crustal basement beneath the Triassic flysch sediments. Combined with the highly enriched Sr and Nd isotopic compositions of the Yanggon and Maoergai granitoids, a remnant Paleo-Tethys oceanic basin, as suggested by Zhou and Graham (1993) and Yin and Nie (1993), is unsuitable to serve as the basement of the Songpan-Garze flysch basin. In the southeastern part of the Songpan-Garze belt, it was proposed that the crustal basement is Proterozoic, which has an affinity to the Yangtze (South China) block (Roger et al. 2004). However, this conclusion is mainly based on the Nd isotopic data of two granitoid samples (Roger et al. 2004). A more extensive study is thus necessary.

Within the Songpan-Garze Triassic flysch basin, no Proterozoic basement is exposed. However, some Proterozoic basements are exposed along the western margin of the Yangtze block (Fig. 1). In those Proterozoic basements, the Kanding complex (796–797 Ma, U–Pb zircon SHRIMP, Zhou et al. 2002), composed of granitic gneiss and amphibolite, is located southeast of the Songpan-Garze belt (western margin of the Yangtze block). The Bikou Group (776–840 Ma, U–Pb zircon SHRIMP, Yan et al. 2003), composed of meta-basic volcanic rocks, is located northeast of the Songpan-Garze belt (northwestern margin of the Yangtze Block).

According to published Nd–Sr isotopic data from the two basements (Yan et al. 2004; Ling et al. 1998; Chen et al. 2000), the Isr and $\varepsilon_{Nd}(t)$ values have been calculated at t = 220 Ma and shown in Fig. 9. The results show that the Bikou Group meta-volcanic rocks with ε_{Nd}(220 Ma) values of > 0 is unlikely to be the magma source for the Yanggon and Maoergai granitoids. The Sr–Nd isotopic compositions for both the granitoids are partly overlapped with those of the Kanding complex (Fig. 9), indicating that the Kanding complex is not the only source for the granitoids. It is possible that the magma source was from mixing between the Kanding complex and other crustal materials. The latter would include the Triassic sediments or the Cambrian–Permian sedimentary cover developed along the western margin of the Yangtze block. Unfortunately, those sediments have Nd isotopic data (Chen et al. 2000) but lack Sr isotopic data. Therefore, we use $^{147}Sm/^{144}Nd$ versus $\varepsilon_{Nd}(t)$ diagram (Fig. 10) to evaluate whether the sediments were mixed with the magma source of the Yanggon and Maoergai granitoids. As shown in Fig. 10, the samples of the granitoids fall between the Kanding complex and the sediments. A reasonable interpretation is thus that the magma source for the Yanggon and Maoergai granitoids was a mixture between the Proterozoic Kanding complex and the sediments, but it is difficult to identify whether the sediments is the Triassic sediment or the Cambrian–Permian sediments of the Yangtze block

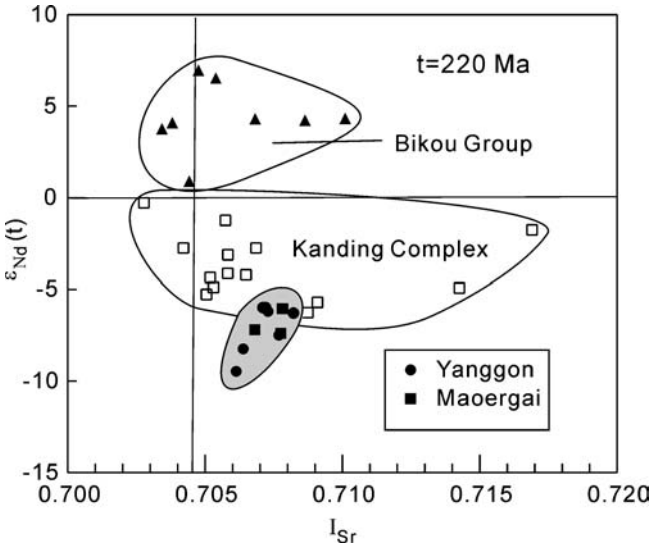

Fig. 9 $\varepsilon_{Nd}(t)$ versus Isr diagram. Data of the Bikou Group are from Yan et al (2004) and data of the Kanding Complex are from (Ling et al. 1998; Chen et al. 2000)

because these sediments have a similar Nd isotopic composition. The mixed source of the Kanding complex and the sediments suggests that the magma generation of the Yanggon and Maoergai granitoids would have taken place in a décollement zone between basement and sedimentary cover. This is in agreement with the large-scale décollement of the Songpan-Garze belt in the late Triassic (Xu et al. 1992). Partial melting of the mixing source could have been promoted by shear heat along the décollement. On the other hand, the magma source composition for the granitoids demonstrates that the basement of the Songpan-Garze belt

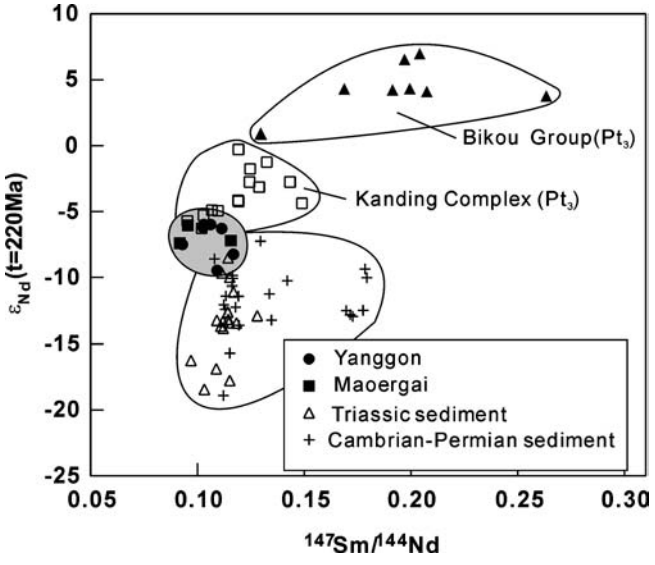

Fig. 10 $\varepsilon_{Nd}(t)$ vs. $^{147}Sm/^{144}Nd$ diagram. Data of Cambrian-Permian sediments are from Chen and Yang (2000). Data of Triassic sediments are from Chen Yuelong's unpublished data. Other data source same as Fig. 9

has an affinity with the Yangtze block and exposed Kanding complex along the western margin of the Yangtze block can be taken as the unexposed basement of the Songpan-Garze belt.

Pb isotopic data for the Yanggon and Maoergai granitoids provides another line of evidence for the Yangtze (South China) affinity of the Songpan-Garze basement. Based on Pb isotopic geochemical mapping of the Mesozoic granitoids from China continental blocks (Zhang 1995), the Mesozoic granitoids from the Yangtze block have a Pb isotopic composition distinct from those of the North China block. Generally, the former is characterized by high radiogenic Pb isotopic composition with $^{206}Pb/^{204}Pb > 17.8$, whereas the latter is characterized by low radiogenic Pb isotopic composition with $^{206}Pb/^{204}Pb < 17.8$. Therefore, the granitoid Pb isotopic composition can serve as a useful basis for discriminating tectonic affinity of blocks. High initial Pb isotopic ratios ($^{206}Pb/^{204}Pb$ = 18.191–18.624, $^{207}Pb/^{204}Pb$ = 15.628–15.685, $^{208}Pb/^{204}Pb$ = 38.317–38.480) of the Yanggon and Maoergai granitoids (Table 4) resemble those of the Yangtze Mesozoic granitoids, but are distinct from those of the North China Mesozoic granitoids (Fig. 11). It is concluded that the basement of the Songpan-Garze belt has an affinity with the Yangtze block.

Tectonic implications

Chronological data of the granitoids provide constraints on tectonic events. Previous study of granitoids in the southeast part of the Songpan-Garze belt showed a time span of tectono-magmatic events ranging from 197 ± 6 Ma to 153 ± 3 Ma, in which the age of 197 ±6 Ma was interpreted as an upper age limit of the Indosinian tectonic event (Roger et al. 2004). Our new U–Pb zircon chronological data show that the Indosinian tectonic event in the Songpan-Garze belt, as represented by the magma crystallization age of the Maoergai pluton, initiated at ~220 Ma (Late Triassic). The new upper age limit of the Indosinian tectonic event in the Songpan-Garze belt accords with the Triassic continental collision between the South China and the North China blocks in Qinling-Dabie-Sulu orogenic belt (East China) (Ames et al. 1996; Hacker et al. 1998; Ayers et al. 2002). Therefore, the Indosinian tectonic event is comprehensive not only in eastern China but also in western China. The convergence between China continental blocks during the Indosinian tectonic event built up the present tectonic framework of China continent blocks.

The Indosinian tectonic event led to the crust of the Songpan-Garze belt being strongly shortened and thickened to > 50 km as revealed by the adakitic Yanggon and Maoergai granitoids. Deep seismic sounding revealed that the present-day crustal thickness of the Songpan-Garze belt is 52–62 km (Wang et al. 2003). We suggest that the crustal thickening of the Songpan-Garze belt started at the Late Triassic. This is distinct from the crustal thickening of the Tibetan Plateau, which started at ~40 Ma (Chung et al. 1998). Therefore, within the range of the Tibetan Plateau (including its eastern adjacent area of the Songpan-Garze belt), the crustal thickening is discordant in time.

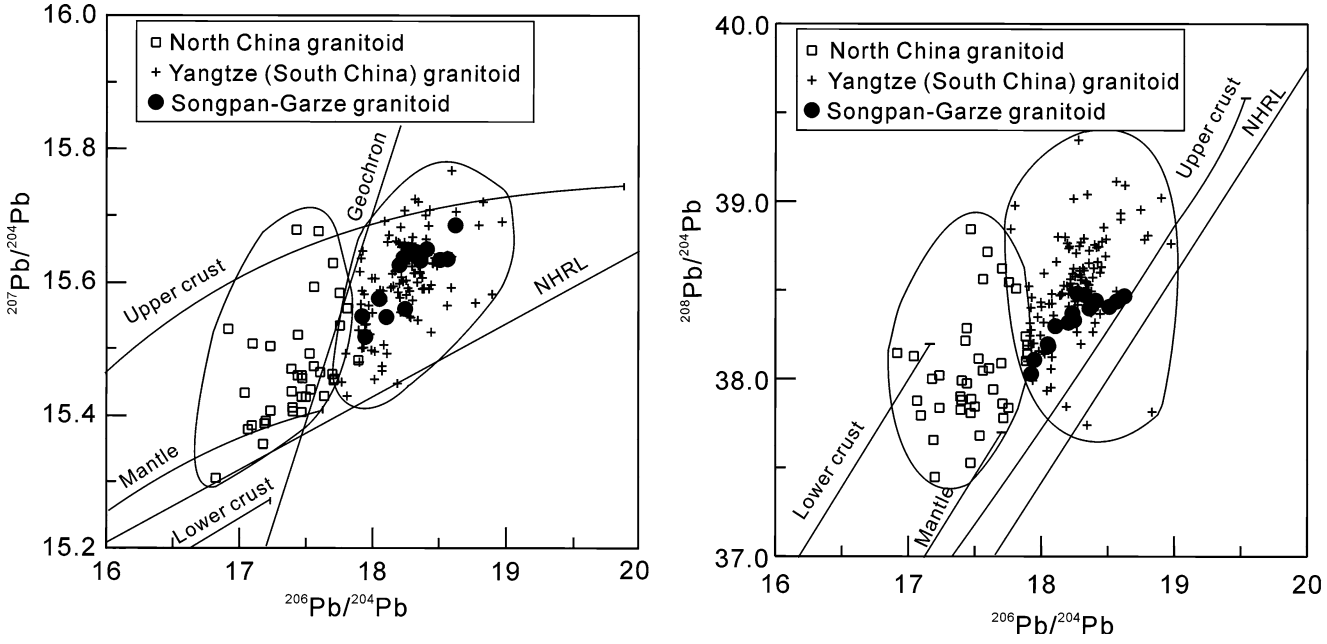

Fig. 11 **a** $^{207}Pb/^{204}Pb$ versus $^{206}Pb/^{204}Pb$ diagram, **b** $^{208}Pb/^{204}Pb$ versus $^{206}Pb/^{204}Pb$ diagram. Data of the North China and Yangtze granitoids are from Zhang (1995), which is K-feldspar Pb isotopic ratios of Mesozoic granitoids. Data of the Yanggon and Maoergai granitoids are whole-rock initial Pb isotopic ratios (see Table 4). Pb isotopic evolution lines of upper crust, lower crust and mantle from Zartman and Doe (1981)

It remains unclear whether the crustal thickening developed from the margin to the interior of the Plateau.

The Songpan-Garze belt is located within the eastern Paleo-Tethys tectonic domain. Its southern and northern boundaries are the A'nimaque-Mianlue suture and the Jinshajian suture, respectively, both of which contain the slice of the Paleo-Tethys oceanic crust (Sun et al. 2002; Xu et al. 2002a, 2004; Elena et al. 2003; Wang et al. 2000). In the Songpan-Garze belt, the identification of the Proterozoic basement under the Triassic sediments indicates that the Proterozoic basement was either an island in the eastern Paleo-Tethys ocean or a peninsula derived from a continental block. Because the Proterozoic basement has an affinity with the Yangtze block and there is no evidence for the existence of a paleo-ocean along the western margin of the Yangtze block, the Proterozoic basement of the Songpan-Garze belt would have been connected to the exposed Proterozoic basement along the western margin of the Yangtze blocks. Accordingly, the Proterozoic basement of the Songpan-Garze belt was a peninsula within the eastern Paleo-Tethys ocean. This implies that the A'nimaque-Mianlue ocean and the Jinshajian ocean formed two branches of the eastern Paleo-Tethys ocean, separated partly by a continental block.

Conclusions

The magma crystallization ages for the Yanggon and Maoergai granitoids from the northeastern part of the Songpan-Garze belt are 221 and 216 Ma, respectively. The age of 221 Ma represents a new upper age limit of the Indosinian tectono-magma event in the Songpan-Garze belt, which is consistent with the collision time between the North China and the South China continental blocks in eastern China. The result demonstrates that the Indosinian tectonic event is comprehensive in China. The Yanggon and Maoergai granitoids have adakitic geochemical signatures, formed by partial melting of the thickened lower crust due to convergence between the west China continental blocks. Combined with their chronological data, the crustal thickening in the Songpan-Garze belt started during the Late Triassic, which is distinct from Tertiary collision of the Tibetan Plateau. The magma source for the Yanggon and Maoergai granitoids consist of a mixed Proterozoic basement and overlying sedimentary cover. Thus, the magma generation was in a décollement zone. This demonstrates that an unexposed Proterozoic basement exists beneath the Triassic sediments of the Songpan-Garze belt. The exposed Proterozoic Kanding complex along the western margin of the Yangtze block would be coupled with the unexposed Proterozoic basement. During development of the Paleo-Tethys ocean, the basement of the Songpan-Garze belt would be a peninsula approaching the Paleo-Tethys ocean from the Yangtze block.

Acknowledgments This study is supported by the National Nature Science Foundation of China (grants: 40234052 and 40521001). We thank Guowei Zhang and Shan Gao for helpful discussions, Mabs Kunka, Peter van Calsteren and Louise Thomas for analytical assistance of Sr–Nd isotopes and Yueshen Wan for helpful guidance of U–Pb zircon SHRIMP dating. The manuscript was improved by J. Ayers. We also thank two anonymous reviewers for their comments.

References

Ames L, Zhou G, Xiong B (1996) Geochronology and geochemistry of ultrahigh-pressure metamorphism with implications for collision of the Sino-Korea Cratons, Central China. Tectonics 15:472–489

Atherton MP, Petord N (1993) Generation of sodium-rich magmas from newly underplated basaltic crust. Nature 362:144–146

Avigad D (1995) Exhumation of the Dabieshan ultrahigh-pressure rocks and accumulation of Songpan-Garze flysch sequence, central China: comment. Geology 23:764–765

Ayers JC, Dunkle S, Gao S, Miller C (2002) Constraints on timing of peak and retrograde metamorphism in the Dabie Shan ultrahigh-pressure metamorphic belt, east-central China, using U–Th–Pb dating of zircon and monazite. Chem Geol 186:315–331

Barnes CG, Petersen SW, Kistler RW, Murray R, Kay MA (1996) Source and tectonic implications of tonalite-trondhjemite magmatism in the Klamath Mountain. Contrib Mineral Petrol 123:40–60

Beate B, Monzier M, Spikings R, Cotton J, Silva J, Bourdon E, Eissen JP (2001) Mio-Pliocene adakite generation related to flat subduction in southern Ecuador: the Quimsacocha volcanic center. Earth Planet Sci Lett 192:561–570

Black LP (2003) TEMORA 1: a new zircon standard for Phanerozoic U–Pb geochronology. Chem Geol 200:155–170

Brugier O, Lancelot JR, Malavieille J (1997) U–Pb dating on single zircon grains from the Triassic Songpan-Garze flysch (Central China): Provenance and tectonic correlations. Earth Planet Sci Lett 152:217–231

Calassou S (1994) Etude tectonique d'une chaine de décollement: A) tectonique Triasique et tertiaire de la chaine de Songpan-Garze. B) géométrie et cinématique des déformations dans les prismes d'accrétion sédimentaire: modélisation analogique. PhD Thesis, Univ. Montpellier II, p 400

Chen SF, Wilson CJL (1996) Emplacement of the Longmen Shan thrust-nappe belt along the eastern margin of the Tibetan Plateau. J Struct Geol 18:413–440

Chen SF, Wilson CJL, Worley BA (1995) Tectonic transition from the Songpan–Garzê fold belt to the Sichuan Basin, southwestern China. Basin Res 7:235–253

Chen YL, Luo ZH, Liu C (2000) Re-recognition on the western margin of the Yangtze craton based on Nd and Pb isotopic compositions. Eos Trans, Western Pacific Geophysics Meet, Suppl V AGU 81:32B–03

Chen YL, Yang ZF (2000) Nd model ages of sedimentary profile from the northwest Yangtze craton, Guangyuan, Sichuan province, China and their geological implication. Geochemical J 34:263–270

Chung SL, Lo CH, Lee TY (1998) Diachronous uplift of the Tibetan Plateau starting 40 My ago. Nature 394:769–773

Chung SL, Dunyi L, Ji J, Chu MF, Lee HY, Wen DJ, Lo CH, Lee TY, Qian Q, Zhang Q (2003) Adakites from continental collision zones: melting of thickened lower crust beneath southern Tibet. Geology 31:1021–1024

Compston W, Williams IS, Kirschvink JL (1992) Zircon U–Pb ages of early Cabbrian time-scale. J Geol Soc149:171–184

Defant MJ, Drummond MS (1990) Derivation of some modern arc magmas by melting of young subducted lithosphere. Nature 34:662–665

Drummond MS, Defant MJ, Kepezhinskas PK (1996) Petrogenesis of slab-derived trondhjemite-tonalite-dacite/adakite magmas. Trans R Soc Edinburgh Earth Sci 87:205–215

Elena AK, Maurice B, Jacques M (2003) Discovery of the Paleo-Tethys residual peridotites along the Anyemaqen–KunLun suture zone (North Tibet). C R Geoscience 335:709–719

Gao S, Rudnick RL, Yuan HL, Liu XM, Liu YS, Xu WL, Ling WL, Ayers J, Wang XC, Wang QH (2005) Recycling lower continental crust in the North China craton. Nature 432:892–897

Gutscher MA, Maury R, Eissen JP, Bourdon E (2000) Can slab melting be caused by flat subduction? Geology 28:535–538

Hacker BR, Ratschbacher L, Webb LE, Ireland TR, Walker D, Dong S (1998) U/Pb zircon ages constrain the architecture of the ultrahigh-pressure Qinling-Dabie orogen, China. Earth Planet Sci Lett 161:215–230

Hou ZQ, Gao YF, Qu XM, Rui ZY, Mo XX (2004) Origin of adakitic intrusives generated during mid-Miocene east–west extension in southern Tibet. Earth Planet Sci Lett 220:139–155

Ling HF, Xu SJ, Shen WZ, Wang RC, Lin YP (1998) Nd, Sr, Pb, O isotopic compositions of Late Proterozoic Gezong and Donggu granites in the west margin of Yangtze plate and comparison with other coeval granitoids (in Chinese with English abstract). Acta Petrologica Sinica 14:269–277

Ludwig KR (1997) Using Isoplot/EX, version 2, in A Geolocronolgical Toolkit for Microsoft Excel. Berkeley Geochronological Center Special Publication 47

Mattauer M, Malavieille J, Calassou S, Lancelot J, Roger F, Hao Z, Xu Z, Hou L (1992) La chaîne triasique de Songpan-Garze (Quest Sechuan et Est Tibet): une chaîne de plissement-décollement sur marge passive. Comptes Rendus de l'Académie des Sciences Paris 314:619–626

Muir RG, Weaver SD, Bradshaw JD, Eby GN, Evans JA (1995) Geochemistry of the cretaceous separation point batholiths, New Zealand: granitoid magmas formed by melting of mafic lithosphere. J Geol Soc 152:689–701

Nie S, Yin A, Rowly Y, Jin Y (1994) Exhumation of the Dabieshan ultrahigh-pressure rocks and accumulation of Songpan-Garze flysch sequence, central China. Geology 22:999–1002

Peacock SM, Rusher T, Thompson AB (1994) Partial melting of subducting oceanic crust, Earth Planet Sci Lett 121:224–227

Petford N, Atherton M (1996) Na-rich partial melts from newly underplated basaltic crust: the Cordillera Blanca batholith. Peru J Petrol 37:1491–1521

Rapp PR, Shimizu N, Norman MD, Applegate GS (1999) Reaction between slab-derived melt and peridotite in the mantle wedge: Experimental constrains at 3.8 Gpa. Chem Geol 160:335–356

Roger F, Malavieille J, Leloup PhH, Calassou S, Xu Z (2004) Timing of granite emplacement and cooling in the Songpan-Garze fold belt (eastern Tibetan Plateau) with tectonic implications. J Asian Earth Sciences 22:465–481

Sajona FG, Maury RC, Pubellier M (2000) Magmatic source enrichment by slab-derived melts in a young post-collision setting, central Mindanao (Philippines). Lithos 54:173–206

Sen C, Dunnt T (1994) Dehydration melting of a basaltic composition amphibolite at 1.5 and 2.0 Gpa: implication for the origin of adakites. Contrib Mineral Petrol 117:394–409

Sengör AMC, Natalin BA (1996) Paleotectonics of Asia: gragment of a synthesis. In: Yin A, Harrison TM (eds) The tectonics of Asia. Cambridge University Press, New York pp 486–640

Sengör AMC (1985) Tectonic subdivisions and evolution of Asia. Bull Technical University Istanbul 46:355–435

Sun SS, McDonough WF (1989) Chemical and isotopic systematics of oceanic basalts: implications for mantle composition and processes. In: Sunders AD, Norry MJ (eds) Magmatism in the Ocean Basins. Special Publications, London 42:313–345

Sun Y, Chen L, Fen GT, Gao M, He YH (2002) A dynamic model of Paleo-Tethyan evolution: evidences from Paleo-Tethyan ophiolite in China (in Chinese with English abstract). J Northwest University 32:1–6

Taylor SR, McLennan SM (1985) The continental crust: its composition and evolution. Blackwell Scientific Publication, Oxford p 132

Wang CY, Han W, Wu JP, Lou H, Bai ZM (2003) Crustal structure beneath the Songpan-Garze orogenic belt (in Chinese with English abstract). Acta Seismologica Sinica 25:229–241

Wang Q, McDermott F, Xu JF, Bellon H, Zhu YT (2005) Cenozoic K-rich adakitic volcanic rocks in the Hohxil area, northern Tibet: Lower-crustal melting in an intracontinental setting. Geology 33:465–468

Wang Q, Xu JF, Jian P, Bao ZW, Zhao ZH, Li CF, Xiong XL, Ma JL (2006) Petrogenesis of adakitic porphyries in an extensional tectonic setting, Dexing, South China: implications for the genesis of porphyry copper mineralization. J Petrol 47:119–144

Wang XF, Metcalfe I, Jian P, He L, Wang C (2000) The Jinshajiang–Ailaoshan suture zone, China: tectonostratigraphy, age and evolution. J Asian Earth Sci 18:675–690

White AJR, Chappell BW (1977) Ultrametamorphism and granitoid genesis. Tectonophysics 43:7–22

Williams I.S, Claesson S (1987) Isotope evidence for the Precambrian province and Caledonian metamorphism of high grade paragneiss from the Seve Nappes, Scandinavian Caledonides, II. Ion microprobe zircon U-Th-Pb. Contrib Mineral Petrol 97:205–217

Xu JF, Castillo PR (2004) Geochemical and Nd–Pb isotopic characteristics of the Tethyan asthenosphere: implications for the origin of the Indian Ocean mantle domain. Tectonophysics 393:9–27

Xu JF, Castillo PR, Li XH, Yu XY, Zhang BR, Han YW (2002a) MORB-type rocks from the Paleo-Tethyan Mian-Lueyang northern ophiolite in the Qinling Mountains, central China: implications for the source of the low $^{206}Pb/^{204}Pb$ and high $^{143}Nd/^{144}Nd$ mantle component in the Indian Ocean. Earth Planet Sci Lett 198:323–337

Xu JF, Shinjo R, Defant MJ, Wang Q, Rapp RP (2002b) Origin of Mesozoic adakitic intrusive rocks in the Ningzhen area of east China: partial melting of delaminated lower continental crust? Geology 30:1111–1114

Xu Z, Hou L, Wang Z (1992) Orogenic process of the Songpan-Garze Orogenic Belt of China (in Chinese with English abstract). Geological Publishing House, Beijing p 190

Yan QR, Andrew DH, Wang ZQ, Yan Z, Peter AD, Wang T, Liu DY, Song B, Jiang CF (2004) Geochemical and tectonic setting of the Bikou volcanic terrane on the northern margin of the Yangtze plate (in Chinese with English abstract). Acta Petrologica et Mineralogica 23:2–11

Yan QR, Wang ZQ, Yan Z, Andraw DH (2003) SHRIMP U–Pb zircon dating constraints on formation time of the Bikou Group volcanic rocks (in Chinese with English abstract). Geol Bull China 22:456–460

Yin A, Nie S (1993) An indentation model for North and South China collision and the development of the Tanlu and Honam fault systems, eastern Asian. Tectonics 12:801–813

Zartman RE, Doe BR (1981) Plumbotectonics–the model. Tectonophysics 75:135–162

Zhou D, Graham SA (1993) Songpan-Garze Triassic complex as a remnant ocean basin along diachronous collision orogen, central China. Geol Soc Am Abst Prog 25:A118

Zhou MF, Yan DP, Kennedy AK (2002) SHRIMP U–Pb zircon geochronological and geochemical evidence for Neoproterozoic arc-magmatism along the west margin of the Yangtze Block, South China. Earth Planet Sci Lett 196:51–67

Zhang GW, Zhang BR, Yuan XC, Xiao QH (2000) Qinling Orogenic belt and continental dynamics (in Chinese with English abstract). Science Press, Beijing p 855

Zhang HF, Gao S, Zhong ZQ, Zhang BR, Zhang L, Hu SH (2002) Geochemical and Sr–Nd–Pb isotopic compositions of Cretaceous granitoids: constraints on tectonic framework and crustal structure of the Dabieshan ultrahigh pressure metamorphic belt, China. Chem Geol 186:281–299

Zhang HF, Harris N, Parrish R, Kelley S, Zhang L, Roger N, Argles T, King J (2004) Cause and consequences of protracted melting of the mid-crust exposed in the North Himalayan antiform. Earth Planet Sci Lett 228:195–212

Zhang LG (1995) Block-geology of Eastern Asia Lithosphere—isotope geochemistry and dynamics of upper mantle, basement and granite (in Chinese with English abstract). Chinese Science Press, Beijing p252